10B.1 THE CHARACTERIZATION OF THE EFFECTS OF ANTENNA POLARIZATION ERRORS ON SIMULTANEOUS HORIZONTAL AND VERTICAL TRANSMIT POLARIZATION DATA

J.C. Hubbert*, S. Ellis, G. Meymaris and M. Dixon
National Center for Atmospheric Research, Boulder CO

1 INTRODUCTION

The simultaneous transmission and reception of H (horizontal) and V (vertical) polarized waves (called SHV mode) has become a very popular way to achieve dual polarization for weather radar (Doviak et al. 2000). One advantage is that a fast polarization switch is not necessary to achieve dual polarization data. The disadvantages are 1) that the linear depolarization ratio (LDR) is not measured and 2) that there can be cross-coupling of the H and V waves which will lead to biases in the polarization variables, particularly Z_{dr} (differential reflectivity). The viability of the SHV technique is base on 1) non-zero mean canting angle of the propagation medium, and 2) negligible antenna polarization errors. If either condition is not met, cross-coupling between the H and V channels occurs which will cause measurement biases.

Measurement errors in the SHV mode have been investigated. Doviak et al. (2000) evaluated cross-coupling errors of SHV mode and concluded that since the mean canting angle of rain is zero, the errors were acceptable. Wang and Chandrasekar (2006) investigated the measurement errors in Z_H (reflectivity), Z_{dr}, ϕ_{dp} (differential phase) and ρ_{hv} (magnitude of the copolar correlation coefficient) due to cross-coupling errors caused by the radar system as a function of ϕ_{dp}. They concluded that system isolation between the the H and V channels must be greater than 44 dB in order to insure that the Z_{dr} bias is with 0.2 dB for worst case errors.

Ryzhkov and Zrnić (2007) examined the effects of non-zero mean canting angle of the precipitation medium on SHV mode measurements. Data gathered in SHV mode with KOUN displayed Z_{dr} radial bias "stripes" after the radar waves passed through the ice phase of either convective cells or stratiform precipitation. They propose that non-zero mean canting angle of the propagation medium causes coupling between the H and V polarized waves that causes the anomalous Z_{dr} signatures.

All reflector type antennas will introduce some distortion to the desired H and V transmit polarization states causing cross coupling between the H and V polarization states. This will bias polarization measurements of precipitation and these errors are similar to the cross-coupling problem reported in Ryzhkov and Zrnić (2007). This paper investigates the impact of antenna induce cross-coupling errors caused by the non ideal radar antenna. The radar model introduced by Hubbert and Bringi (2003) is used to quantify the impact of polarization errors on Z_{dr} and ϕ_{dp}. Transmit errors are also included separately in the model by specifying the transmit polarization state that is fed to the antenna. Finally experimental data from S-Pol, NCAR's S-band polarimetric radar, and KOUN, NSSL's experimental S-ban radar, are used to illustrate the theory. Recently, S-Pol collected data in fast alternating H and V mode (referred to as FHV mode) quickly followed by data collected in simultaneous H and V transmit mode. These data clearly illustrate the effects of antenna polarization errors.

2 ANTENNA ERRORS

Antenna errors are quantified in the model by the complex numbers ξ_h and ξ_v (Hubbert et al. 2009). These errors can be equivalently defined by the tilt and ellipticity angles, i.e., $\alpha_{h,v}$ and $\epsilon_{h,v}$ respectively, of the polarization ellipse as shown in Fig. 1. E_h and E_v are the horizontal and vertical electric field components. Ideally if only an H polarized field is sent to the antenna, only H polarization would emerge from the antenna and be propagated into space. This pure H polarized wave would be represented as a horizontal line on the H axis of Fig. 1. However, due to the non-ideal feedhorn and antenna dish, some of the H polarized wave is coupled to the V channel. This error is characterized by the complex number ξ_h and is equivalently represented by the tilt and ellipticity angles α_h and ϵ_h, respectively. Similarly for the vertical channel, ξ_v is the antenna error which can be equivalently represented by α_v and ϵ_v. Mathematically,

$$\begin{bmatrix} E_h^{rad} \\ E_v^{rad} \end{bmatrix} = \begin{bmatrix} i_h & \xi_v \\ \xi_h & i_v \end{bmatrix} \begin{bmatrix} E_h^t \\ E_v^t \end{bmatrix} \quad (1)$$

where E_h^t and E_v^t are the electric fields input to the OMT and feedhorn and E_h^{rad} and E_h^{rad} are the electric fields radiated into free space, and $i_{h,v}$ are real numbers such that $|\xi_h|^2 + i_h^2 = 1$ and $|\xi_v|^2 + i_v^2 = 1$. Representing

*NCAR/EOL, Boulder, Colorado 80307, email: hubbert@ucar.edu

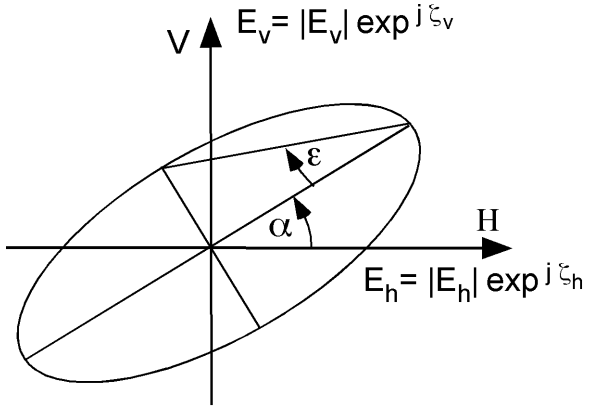

Figure 1: *The polarization ellipse. Propagation is into the paper.*

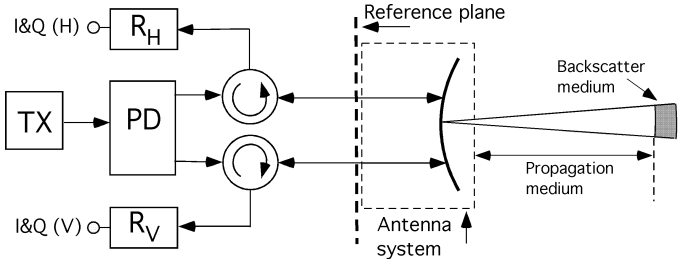

Figure 2: *A block diagram showing the elements of the radar model. TX is the transmitter block, PD is the power division network and R_H and R_V are the vertical and horizontal receiver chains.*

the antenna polarization errors in terms of the the tilt and ellipticity angles provides insight as to the character of the antenna errors.

A description of the radar scattering model can be found in Hubbert et al. (2009); Hubbert and Bringi (2003). First the model is used to illustrate the different effects that tilt and ellipticity angle errors individually have on Z_{dr} bias. Figure 3 shows Z_{dr}^{shv} for one-degree, orthogonal polarization tilt errors (upper panel) and one-degree orthogonal polarization ellipticity errors (lower panel), both versus ϕ_{dp}^P, principal plane ϕ_{dp} (see Hubbert et al. (2009) for a discussion of ϕ_{dp}^P). The θ (mean canting angle of the propagation medium) is zero and $E_v^t = E_h^t$ ($E_{h,v}^t$ are the H and V electric fields input to the antenna at the reference plane (See Fig. 2). The magnitude of these errors, i.e, $|\xi_h + \xi_v|$, corresponds to an LDR system limit of about -30 dB. The solid straight lines represent non-biased Z_{dr} that would be measured in fast alternating H and V transmit mode. The figure shows that Z_{dr} bias is significant with a maximum error of about 0.6 dB when $\phi_{dp}^P = 180°$.

It is likely that true antenna errors will be some combination of tilt and ellipticity angle errors and thus we present the following again as an illustrative example of how antenna errors affect Z_{dr}^{shv}. Figure 4 shows Z_{dr}^{shv} bias for the H and V tilt and ellipticity error angles given in Table 1. The antenna errors are orthogonal, i.e., $\xi_v = -\xi_h^*$. The figure shows that the character of the Z_{dr} bias is quite different for each curve with a maximum bias about 0.4 dB. These antenna errors all correspond to about a -31 dB LDR system limit.

These same antenna errors from Table 1 are used again in Fig. 5, but for circular transmit polarization. The Z_{dr} biases curves have changed dramatically and demonstrate the importance of the phase difference between the H and V components of the transmit wave. The transmit wave is defined here at the reference plane shown in Fig. 2.

As shown in Hubbert et al. (2009), S-Pol's antenna polarization errors are fairly well characterized by orthogonal ellipticity angles and by H and V tilt angles of $0°$ and $90°$, respectively, (i.e., no tilt angle errors). Using this restriction, for an LDR system limit value, the ellipticity error angle can be calculated. Table 2 gives the error ellipticity angles for several LDR system limit values. The corresponding values for the $Im\{\xi_h\}$ (or equivalently ϵ_h in radians) are also given.

We next examine SHV K_{dp} biases caused by polarization errors given in Table 3. These antenna polarization errors correspond to a LDR system limit of -25 dB. Shown in Fig. 6 is K_{dp}^{shv}/K_{dp}^P as a function of principal plane ϕ_{dp}. The K_{dp} bias is fairly small, always being less than 3%. If the LDR system limit is less than -30 dB, the K_{dp} error is within 2%.

The biases of SHV ρ_{hv} for LDR system limits as high -25 dB are less than 1% and are not plotted.

3 SHV Z_{dr} AS A FUNCTION OF LDR SYSTEM LIMIT

As shown in Hubbert et al. (2009), the antenna polarization error terms appear as $\xi_h + \xi_v$ in the expression for LDR system limit and SHV Z_{dr} in drizzle. Thus, the LDR system limit for a radar can be related to the SHV Z_{dr} bias as a function of ϕ_{dp}^P with differential transmit phase as a parameter. Based on the antenna errors for S-Pol, the antenna errors are modeled as orthogonal ellipticity angles with no tilt angle errors. This is shown in Fig. 7 for (a) slant 45° linear transmit polarization (i.e., $E_h^t = E_v^t$) and (b) circular transmit polarization. The shown ϵ denotes the sign of the H polarization ellipticity angle. The values of the ellipticity angle corresponding to each curve are given in Table 2. Note how not only the shape of bias curves changes but also the maximum Z_{dr} bias increases significantly for circular transmit polariza-

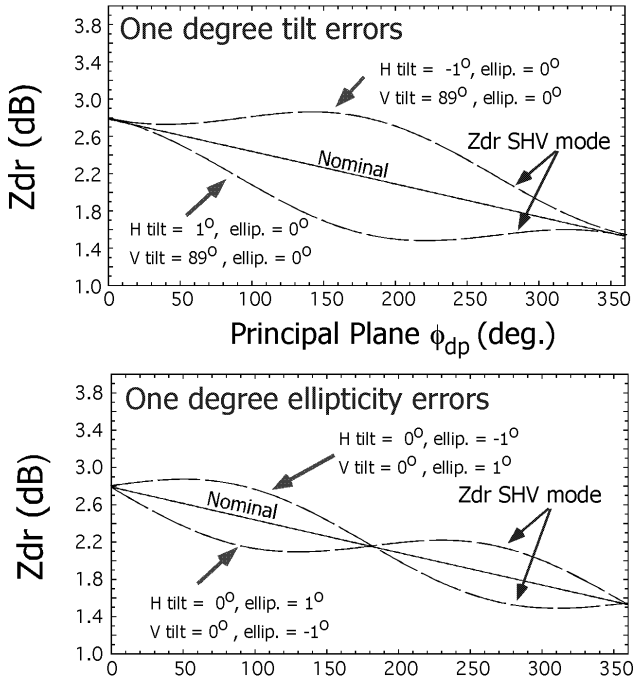

Figure 3: *SHV mode Z_{dr} for one degree antenna polarization errors. The upper panel shows $\pm 1^\circ$ tilt errors while the lower panel shows $\pm 1^\circ$ ellipticity errors.*

	H tilt	H ellip.	V tilt	V ellip.
A	-0.5°	-0.7°	89.5°	0.7°
B	0.5°	-0.7°	90.5°	0.7°
C	-0.5°	0.7°	89.5°	-0.7°
D	0.5°	0.7°	90.5°	-0.7°

Table 1: *The H and V tilt and ellipticity error angles corresponding to Fig. 4.*

tion. The model shows that the most stringent crosspolar isolation criteria results for the circular polarization transmit condition. As can be seen, if SHV Z_{dr} bias is to be kept under 0.2 dB, the LDR system limit needs to be about -40 dB. Practically, if one of the circular transmit bias curves characterized a radar, the Z_{dr} bias at $\phi_{dp} = 0$ would likely be detected by the user and a Z_{dr} offset correction factor would be used. Then, the maximum Z_{dr} bias would occur for $\phi^P_{dp} = 180^\circ$ instead of at $\phi^P_{dp} = 0^\circ$.

4 S-Pol EXPERIMENTAL SHV DATA

During May and June of 2008, S-Pol was deployed in Southern Taiwan for the field experiment TiMREX (Terrain-influenced Monsoon Rainfall Experiment). S-Pol was operated in the FHV (fast alternating H and V

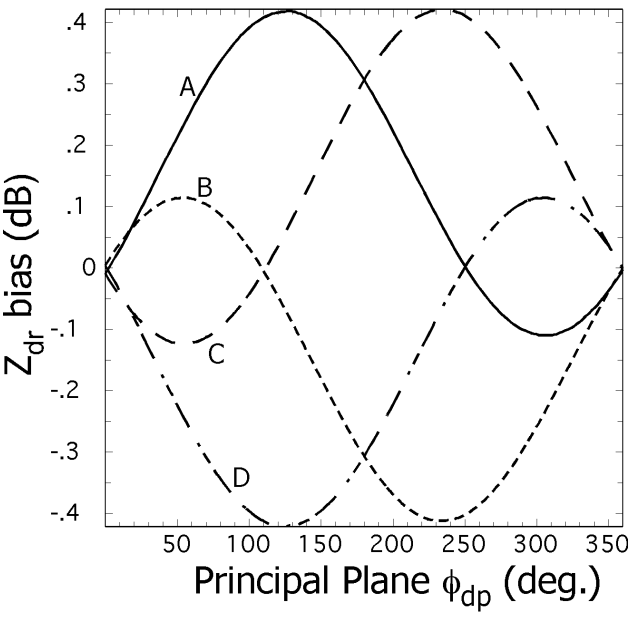

Figure 4: *SHV mode Z_{dr} for mixed tilt and ellipticity antenna error angles which are given in Table 1. The antenna errors are orthogonal and the H and V transmit signals are equal, i.e., $E_h = E_v$. These antenna errors correspond to a system LDR limit of -31 dB.*

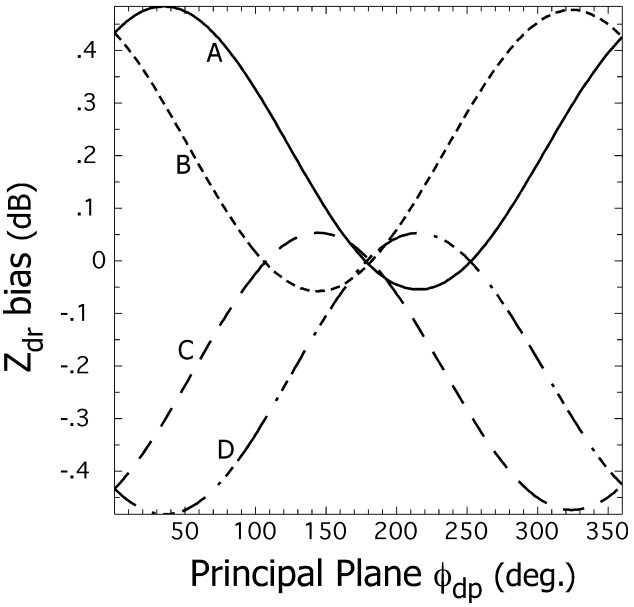

Figure 5: *SHV mode Z_{dr} for mixed tilt and ellipticity antenna error angles which are given in Table 1, however, the transmission polarization state is circular. The antenna errors are orthogonal. These antenna errors correspond to a system LDR limit of -31 dB.*

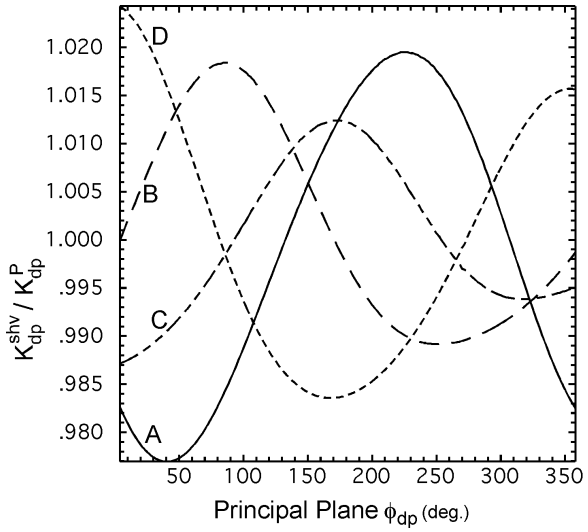

Figure 6: *Normalized SHV mode K_{dp} as a function of principal plane ϕ_{dp} for the antenna error angles given in Table 3.*

	LDR (dB)	$\Im\{\xi_h\} \approx \epsilon$ (rad.)	ϵ (deg.)
A	-25	0.0281	1.61°
B	-30	0.016	0.91°
C	-35	0.009	0.509°
D	-40	0.005	0.286°
E	-45	0.003	0.161°

Table 2: *Antenna polarization errors as a function of system LDR limit. The antenna errors are assumed to be orthogonal and elliptical.*

	H tilt	H ellip.	V tilt	V ellip.	trans. pol.
A	0°	1.61°	90°	-1.61°	linear
B	0°	-1.61°	90°	1.61 °	linear
C	0°	1.61°	90°	-1.61°	circular
D	0°	-1.61°	90°	1.61°	circular

Table 3: *The H and V tilt and ellipticity error angles corresponding to Fig. 6. The corresponding LDR system limit is -25 dB.*

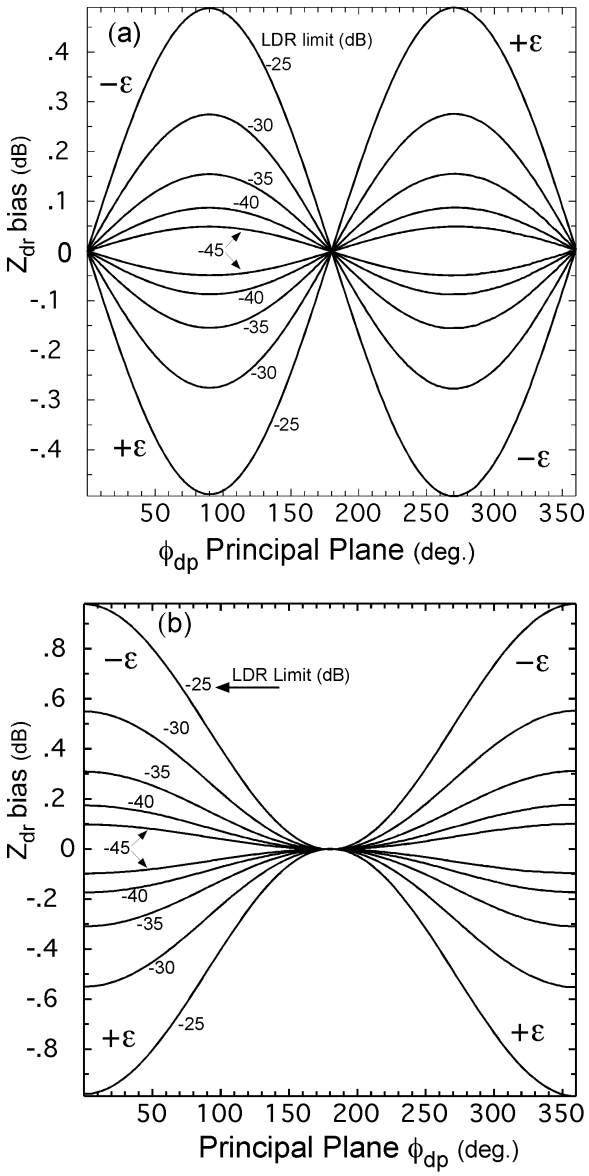

Figure 7: *SHV mode Z_{dr} bias as a function of principal plane ϕ_{dp} with LDR system limit as a parameter. The antenna polarization errors are assumed to be orthogonal ellipticity angles. The sign of the H ellipticity angle is given in each quadrant. (a) The transmit polarization is $45°$ linear, i.e., $E_h^t = E_v^t$. The curves all mimic a sine wave shape. (b) The transmit polarization is circular. The curves are symmetric about the vertical line through $180°$. The corresponding antenna errors are given in Table 2.*

polarization) transmit mode for the majority of the project (normal operation mode), however, limited data were collected in the SHV (simultaneous H and V transmit) mode interleaved with the FHV data. Thus, SHV and FHV data that were gathered only minutes apart can be compared. Higher elevation PPIs illustrate radial Z_{dr}^{shv} bias stripes similar to the ones shown in Ryzhkov and Zrnić (2007) caused by canted ice-phase particles. See Hubbert et al. (2009) for a discussion of the TiMREX higher elevation cuts.

Figures 8 and 9 show S-Pol FHV mode reflectivity (Z) and differential reflectivity (Z_{dr}) gathered during TiMREX on 2 June 2008, 6:17:06 UTC at 2.0° elev. Figures 10, 11 and 12 show SHV Z , Z_{dr} and ϕ_{dp} gathered at 6:11:28 UTC at 2.0° elev. The SHV and FHV Z_{dr} data appear fairly comparable but in fact there is a bias in the SHV data. To show this, we employ the self consistency Z calibration technique of Vivekanandan et al. (2003). The technique is based on the relationship of Z, Z_{dr} and ϕ_{dp} in rain. Assuming a typical range of rain drop size and shape distributions, ϕ_{dp} can be estimated from measured Z and Z_{dr}. This estimated ϕ_{dp} (ϕ_{dp}^{e}) is compared to the measured ϕ_{dp} (ϕ_{dp}^{m}). A scatter plot is generated and a straight line fit is calculated. If the calculated mean line differs from the 1-to-1 line, this indicates a reflectivity bias. The technique assumes that Z_{dr} is well calibrated (S-Pol Z_{dr} is calibrated via vertical pointing data in light rain). The self-consistancey technique can also be used to investigate Z_{dr} bias as is done below.

Shown in Fig.13 is a scatter plot of ϕ_{dp}^{e} versus ϕ_{dp}^{m} for TiMREX data. The Z bias is about 0.03 dBZ, i.e., negligible. Note the tight scatter about the 1-to-1 line. This indicates that S-Pol is well calibrated and such self consistency plots are the norm for S-Pol. Fig. 14 is similar to Fig. 13 except the data was gathered in SHV mode. The scatter is rather tight about the 1-to-1 line for $\phi_{dp} < 50°$ but for $\phi_{dp} > 70°$ the computed ϕ_{dp} are biased low. This is due to Z_{dr} bias caused by antenna errors.

To further illustrate this SHV Z_{dr} bias, Z_{dr} is averaged under the constraint 20 dBZ$< Z \leq$ 25 dBZ. These Z_{dr} data are partitioned into three categories: 1) $20° < \phi_{dp} < 40°$, 2) $40° < \phi_{dp} < 70°$, and 3) $70° < \phi_{dp} < 100°$. The results are given in Table 4. For low ϕ_{dp} the SHV and FHV Z_{dr} values are about equal. For $40° < \phi_{dp} < 70°$, the Z_{dr}s differ by 0.11 dB and for $70° < \phi_{dp} < 100°$ the Z_{dr}s differ by 0.27 dB. The data is not corrected for differential attenuation (which could potentially add error). This increasing difference between FHV and SHV Z_{dr} as a function of ϕ_{dp} is consistent with the Z_{dr} bias predicted for antenna errors of radar systems with LDR limit in the -30 dB to -35 dB range.

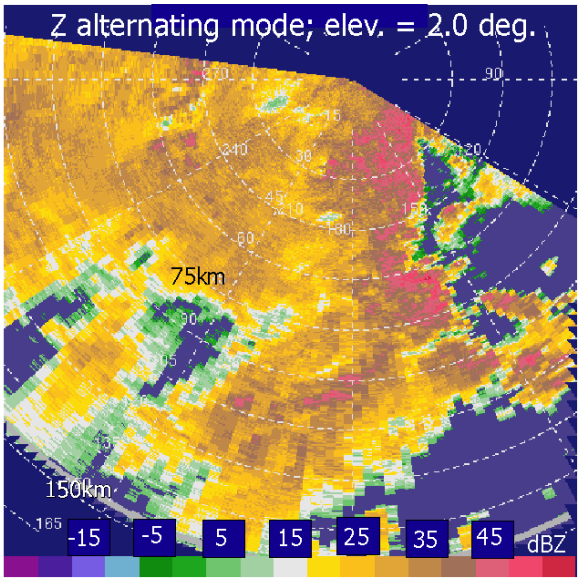

Figure 8: *FHV mode PPI reflectivity for 2.0° elevation. Data were gathered by S-Pol on 2 June 2008 at 06:17:06 UTC during the the Field Campaign TiMREX in southern Taiwan. Range rings are in 15 km increments.*

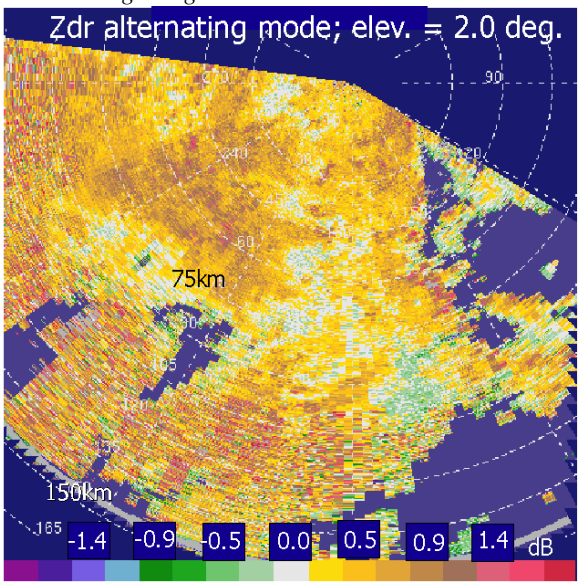

Figure 9: *FHV mode PPI Z_{dr} for 2.0° elevation corresponding to Fig. 8.*

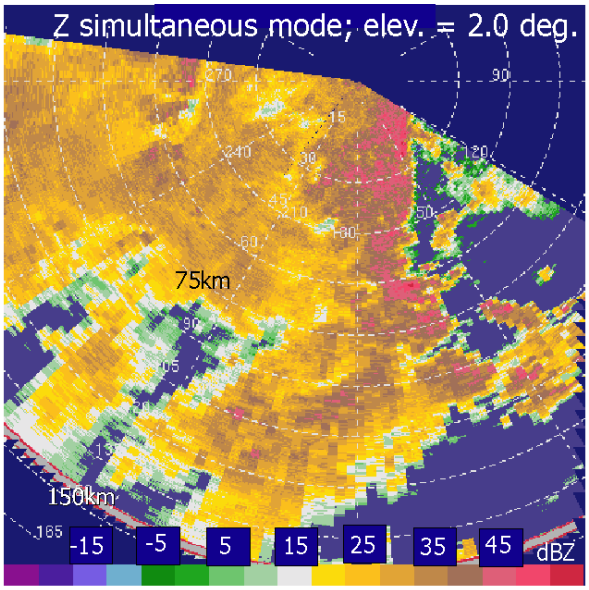

Figure 10: *SHV mode PPI reflectivity for 2.0° elev. Data were gathered by S-Pol on 2 June 2008 at 06:11:28 UTC during the the Field Campaign TiMREX in Southern Taiwan. Range rings are in 15 km increments.*

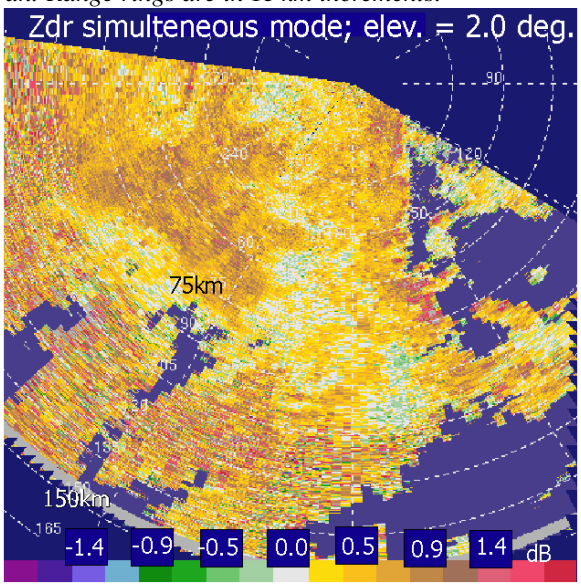

Figure 11: *SHV mode PPI Z_{dr} for 2.0° elev. corresponding to Fig. 10.*

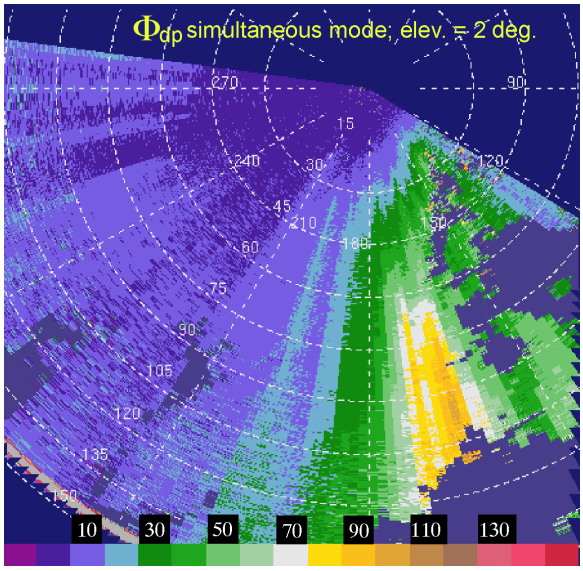

Figure 12: *SHV mode PPI ϕ_{dp} for 2.0° elevation corresponding to Fig. 8.*

5 QUANTIFYING AND CORRECTING Z_{dr} BIAS CAUSED BY ANTENNA ERRORS

The antenna polarization errors, ξ_h and ξ_v, are difficult to quantify and are not typically given by the manufacturer. The errors can be estimated, however, from radar data as shown in Hubbert et al. (2009). The technique uses an estimate of the LDR system limit and solar scan data. The S-Pol antenna polarization errors, in terms of tilt and ellipticity of the polarization ellipse, are $\alpha_h = 0°$, $\epsilon_h = -0.91°$ and $\alpha_v = 90°$, $\epsilon_v = 0.69°$ which corresponds to $\xi_h = -j0.0159$ and $\xi_v = -j0.0120$. These estimated antenna errors are now used in the radar scattering model and the results are shown in Fig. 15. There are no transmit errors (i.e., $E_h^t = E_v^t$, (see Hubbert et al. (2009))), the mean canting angle of the propagation medium is zero, and the backscatter medium is drizzle. As is seen, the Z_{dr} bias becomes more positive with increasing ϕ_{dp} in a similar fashion to that in the above experimental data. The model also predicts that in FHV mode, the measured LDR_h (LDR for H polarization transmission) *decreases* with increasing ϕ_{dp} instead of increasing due to differential attenuation as normally expected. This type of LDR_h behavior is observed with S-Pol data for long paths of increasing ϕ_{dp}. Thus, the model predicts well the general behavior of the observed SHV Z_{dr} bias and FHV LDR_h. A more precise estimate of the antenna errors could be made if the transmit polarization state could be measured and if the differential phase shift incurred from the reference plane to the I and Q samples were determined. While in principle this can be done, in practice it is not

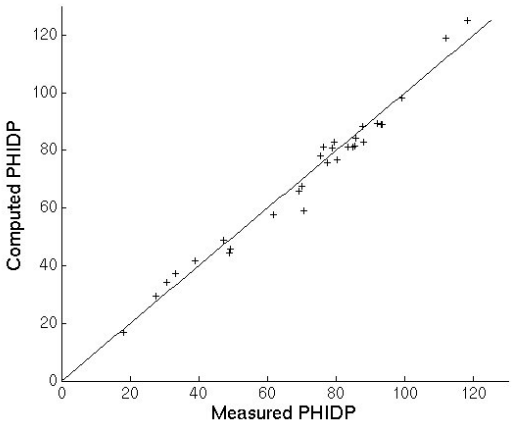

Figure 13: *Scatter plot of calculated ϕ_{dp} (from Z and Z_{dr}) versus measured ϕ_{dp} from TiMREX FHV data corresponding to Figs. 8 and 9. The Z bias is about 0.03 dBZ.*

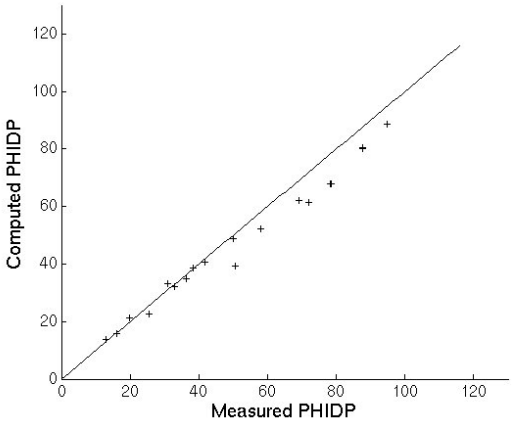

Figure 14: *Scatter plot of calculated ϕ_{dp} (from measured Z and Z_{dr}) versus measured ϕ_{dp} from TiMREX SHV data. Data above approximately 50° are biased low (consistently fall below the ono-to-one line). This is a manifestation of the Z_{dr} bias caused by antenna polarization errors.*

straight forward. To do this, the impedance mismatch of the measurement system and waveguide coupler to the radar system would need to be determined. This would require a vector network analyzer and such a measurement was not attempted. However, the present analysis demonstrates the magnitude and the characteristics of antenna polarization errors and their deleterious effect on SHV mode Z_{dr}.

Finally, the SHV experimental data of Fig. 14 are corrected using the the modeled Z_{dr} bias values from Fig. 15 as a function of measured ϕ_{dp}. The self consistency technique is then again applied to the corrected data and the result is shown in Fig. 16. As can be seen the data are now better clustered around the one-to-one line as compared to the uncorrected data of Fig. 14.

6 KOUN DATA

The following section uses data gathered by KOUN, NSSL's (Nation Severe Storms Laboratory) S-band research radar, on 30 March 2007 through a convective line that produced over 300° of ϕ_{dp} accumulation and serves as another example of SHV Z_{dr} bias caused by antenna polarization errors. This rain event was described by local meteorologists as being more tropical in nature with fewer large drops than typically occur in Oklahoma rain storms[1]. This is confirmed by the National Weather Service sounding data for the time period that shows a moist profile through a deep layer, low vertical wind shear, and relatively low convective available potential energy (CAPE = 834 J). Furthermore there were no hail reports in Oklahoma from the National Weather Service or the Community Collaborative Rain, Hail and Snow Network (CoCoRaHS). Thus, this is an excellent data set for the analysis of antenna polarization errors. The KOUN antenna is similar to the antennas used on the NWS's operational radars (i.e., NEXRAD) except it has a dual-polarized feed horn. It has a center-fed parabolic reflector with three support struts. The $1.5°$ elevation angle data are used in our analysis to avoid the influence of partial beam blockage.

Since KOUN does not operate in FHV mode, only the SHV data are available and no FHV mode data are available for comparison. Nevertheless, the self consistency Z calibration technique can be used to ascertain the presence of Z_{dr} bias due to cross-coupling between the H and V channels. To calibrate KOUN data, PPI plots of Z and Z_{dr} are inspected in regions of light rain/drizzle with low reflectivity and very low ϕ_{dp} accumulation so that intrinsic Z_{dr} should be about 0 dB. From this data,

[1]Personal communications with Terry Schuur Ph.D., of the Cooperative Institute for Mesoscale Meteorological Studies, University of Oklahoma, Norman Oklahoma.

the Z_{dr} bias is estimated to be 0.6 dB. Next, using the self consistency principle, the scatter plot of ϕ^c_{dp} versus ϕ^m_{dp} is calculated using only data with ϕ^m_{dp} less than 50°, which yields a Z bias of 4.7 dB. To verify these estimated calibration numbers, a scatter plot of Z_{dr} versus Z is made for data with $\phi_{dp} < 30^\circ$ (to minimize possible bias caused by the antenna polarization errors) and is shown as the solid line in Fig. 17. The experimental data are put into 5 dBZ bins, averaged, and then standard deviations are calculated. The mean and standard deviation are calculated in linear units and converted back to dB (see Rinehart (2004) for details). The solid vertical lines represent the standard deviations plotted at the midpoints of the 5 dB bins. For comparison, the curve found by Illingworth and Caylor (1989) is plotted in Fig. 17 as the dashed line. The corrected data compare well with the line from Illingworth and Caylor (1989).

The method of Vivekanandan et al. (2003) is applied to the KOUN data calibrated as described above. Once again, the scatter plot of ϕ_{dp} calculated from Z and Z_{dr} versus measured ϕ_{dp} should cluster around the one-to-one line. Figure 18 shows this plot for the KOUN data. The data points are clustered around the one-to-one line for measured ϕ_{dp} less than about 50° but data points are biased low for measured ϕ_{dp} greater than about 50°. Since there are no reference FHV data for comparison, data self consistency is used to demonstrate the Z_{dr} bias in the KOUN data.

The Z_{dr} attenuation correction as well as the Z correction for attenuation will affect the nature of the scatter and there is a degree of uncertainty to these corrections. However, Vivekanandan et al. (2003) show that the scatter plots of ϕ^m_{dp} versus ϕ^e_{dp} for both 1) poorly calibrated Z data and 2) non-attenuation corrected data remain scattered about a mean straight line which has a significantly different slope as compared to 1. Thus, if the scatter of ϕ^e_{dp} versus ϕ^m_{dp} do not cluster well about a straight line, this indicates a Z_{dr} bias caused by antenna polarization errors. Assuming that the KOUN data are well calibrated for data where $\phi^m_{dp} < 50^\circ$, the data of Fig. 18 shows a negative bias of the ϕ^e_{dp} for $\phi^m_{dp} > 50^\circ$. This in turn indicates that Z_{dr} is biased high (see Eq.(16) of Vivekanandan et al. (2003)).

7 ESTIMATING KOUN ANTENNA POLARIZATION ERRORS

While it is impossible to calculate the KOUN antenna polarization errors, as was done for S-Pol, a rough estimate can be made based on the data displayed in Fig 18 using trial and error and the model described in Part I. The antenna polarization error parameters are varied and the model is used to generate Z_{dr} bias curves. The KOUN Z_{dr} is then corrected and scatter plots of ϕ^e_{dp} versus ϕ^m_{dp} are calculated. The Z_{dr} bias curve that best aligns the scatter of such plots around the one-to-one line is judged to yield the best estimate of the KOUN antenna errors. This Z_{dr} bias curve is shown in Fig. 19 and the antenna errors are $\alpha_h = 1.7^\circ$, $\epsilon_h = -0.7^\circ$, $\alpha_v = 91.7^\circ$ and $\epsilon_v = 0.7^\circ$. The transmit polarization ellipse is characterized by $\alpha = 45^\circ$ and $\epsilon = -30^\circ$. The true KOUN antenna errors may be significantly different and still result in a similar Z_{dr} bias curve as Fig. 19. Nevertheless, inevitably KOUN does possess antenna polarization errors as all center-fed parabolic antennas must. Furthermore, the magnitude of the errors must significantly bias SHV Z_{dr} as evidenced by the radar model given in Part I, unless the crosspolar isolation is better than 40 dB. Without a concerted design and development effort, this is extremely unlikely.

The suggested Z_{dr} bias correction curve of Fig. 19 is now used to correct the KOUN Z_{dr} data. As can be seen in Fig. 20, the character of the self consistency plot has improved: the scatter points are now more closely distributed around the one-to-one line as compared to the uncorrected data of Fig. 18. Thus, these estimated antenna errors are judged to be reasonable approximations of the true KOUN antenna errors.

Additional evidence of the validity of the antenna error corrections is provided by Figs. 21 and 22. The data in both figures were corrected for attenuation and differential attenuation using Eqs. (17) and (18) from Vivekanandan et al. (2003). Figure 21 shows a scatter plot of uncorrected mean Z_{dr} versus Z in 5 dB reflectivity bins for $\phi_{dp} > 175^\circ$ (thick solid line) and $\phi_{dp} < 175^\circ$ (thin solid line) . The relationship of Illingworth and Caylor (1989) is again plotted as the dashed line in both Figs. 21 and 22. Figure 22 is similar to Fig. 21 except Z_{dr} has now been corrected for antenna polarization errors by using the curve from Fig. 19. Figure 21 shows that the thin and thick plotted lines are significantly above and below, respectively, the theoretical dashed curve. The observed bias is consistent with Z_{dr} being biased high for data where ϕ_{dp} is less than 175° and being biased low for data where where ϕ_{dp} is greater than 175° as predicted by Fig. 19. In comparison, the corrected data of Fig. 22 now yields curves that are much more consistent and agree with the theoretical curve of Illingworth and Caylor (1989). Note that there are less data available with ϕ_{dp} greater than 175° than less than 175°, resulting in the smaller data coverage of the thick black lines in Figs. 21 and 22.

8 SUMMARY AND CONCLUSIONS

Simultaneous transmission of H and V polarized waves (termed SHV mode) is now a popular way to construct

dual-polarization radar systems largely because of lower cost and technical simplicity: an expensive, fast, high-power polarization switch is avoided. This paper has shown that data quality issues will likely limit the cost-benefit of the SHV technique unless antenna polarization errors can be reduced so that the crosspolar isolation is better than 40 dB, a figure difficult to achieve for center-fed parabolic reflector antennas.

S-Pol data from TiMREX (Terrain-influenced Monsoon Rainfall Experiment) and from KOUN were used to demonstrate the Z_{dr} bias in rain. The S-Pol SHV data were compared to FHV (fast alternating H and V transmit) data which is relatively free of biases caused by inter-channel cross-coupling (Wang and Chandrasekar 2006). S-Pol SHV mode Z_{dr} bias was shown to be about 0.3 dB after about 80° of ϕ_{dp} accumulation in pure rain. Fortunately, small antenna polarization errors such as those found on S-Pol, do not significantly bias K_{dp} nor ρ_{hv}. For the antenna errors considered in this paper, the radar model showed that biases in K_{dp} or ρ_{hv} are both within about 3% of their nominal unbiased values.

SHV radar data from KOUN were also analyzed for antenna polarization errors. This was more difficult since there was no FHV truth data for comparison. Nevertheless, the antenna polarization errors were estimated using the radar model, the principle of self consistency among Z, Z_{dr} and ϕ_{dp} and $Z - Z_{dr}$ scatter plots. The KOUN data analyzed contained over 300° of accumulative ϕ_{dp} and therefore was an excellent case to examine for Z_{dr} bias in rain caused by antenna polarization errors. Using the radar model, Z_{dr} biases were shown to be positive (about 0.5 dB maximum) for $\phi_{dp} < 180°$ and to be negative (about -0.5 dB minimum) for $\phi_{dp} > 180°$.

Mitigation of the SHV mode Z_{dr} bias caused by antenna errors will be difficult. First of all they are very difficult to quantify precisely. If the errors were known exactly, then the data could be corrected. This would only be valid in regions of homogeneous distributions of precipitation particles since antenna errors are not constant across the antenna beam. Thus, reflectivity gradients will affect the magnitude of the Z_{dr} bias. Additionally, radome seams and irregularities as well as radome wetting will also cause polarization errors and measurement biases. Such errors were not considered here (S-Pol operates without a radome hence is free of these errors). The most promising path to reduction of the SHV mode Z_{dr} bias is to reduce the antenna polarization errors via antenna design. However, our model shows that if Z_{dr} bias is to be kept below 0.2 dB, assuming antenna polarization errors are similar in character to S-Pol's antenna errors, the system LDR limit must be reduced to about -40 dB. This is largely in agreement with Wang and Chandrasekar (2006) who quote a similar requirement of -44 dB system LDR limit. Our estimated antenna errors are not worst case as was used by Wang and Chandrasekar (2006). Such a low LDR limit figure may not be cost-effective to achieve with center-feed parabolic antennas and this cost must be considered against the afore-mentioned cost-benefits of implementing SHV mode dual-polarization.

Acknowledgment This research was supported in part by the ROC (Radar Operations Center) of Norman OK. The National Center for Atmospheric Research is sponsored by the National Science Foundation. Any opinions, findings and conclusions or recommendations expressed in this publication are those of the author(s) and do not necessarily reflect the views of the National Science Foundation.

References

Hubbert, J. and V. Bringi, 2003: Studies of the polarimetric covariance matrix: Part II: Modeling and polarization errors. *J. Atmos. Oceanic Technol.*, 1011–1022.

Hubbert, J., S. M. Ellis, G. Meymaris, and M. Dixon: 2009, Cross-coupling, antenna errors and simultaneous horizontal and vertical polarization transmit data. *Preprints, 34th AMS Conf. on Radar Meteorology*, AMS, Williamsburg, VA.

Illingworth, A. and I. Caylor, 1989: Polarization radar estimates of raindrop size spectra and rainfall rates. *J. Atmos. Oceanic Technol.*, **6**, 939–949.

Rinehart, R., 2004: *Radar for meteorologists*. Rinehart Publications, Columbia, MO, 482 pp.

Ryzhkov, A. and D. Zrnić, 2007: Depolarization in ice crystals and its effect on radar polarimetric measurements. *J. Atmos. Oceanic Tech.*, **24**, 1256–1267.

Vivekanandan, J., G. Zhang, S. Ellis, D. Rajopadhyaya, and S. Avery, 2003: Radar reflectivity calibration using differential propagation phase measurement. *Radio Sci.*, **38**, 8049.

Wang, Y. and V. Chandrasekar, 2006: Polarization isolation requirements for linear dual-polarization weather radar in simultaneous transmission mode of operation. *IEEE Trans. Geosc. and Remote Sen.*, **44**, 2019–2028.

Total ϕ_{dp}	Mean Z_{dr} (dB)	
	FHV	SHV
between 20 and 40 deg.	0.17	0.16
between 40 and 70 deg.	0.15	0.26
between 70 and 100 deg.	-0.07	0.20

Table 4: *A comparison of Z_{dr} values for FHV and SHV modes as a function of ϕ_{dp}. Reflectivities are limited to between 20 and 25 dBZ.*

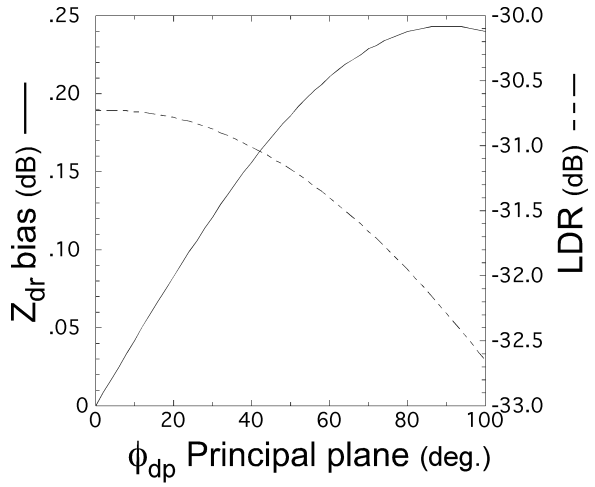

Figure 15: *SHV mode Z_{dr} and FHV mode LDR_h from the model. The antenna polarization errors are $\alpha_h = 0°$, $\epsilon_h = -0.91°$ and $\alpha_v = 90°$, $\epsilon_v = 0.69°$.*

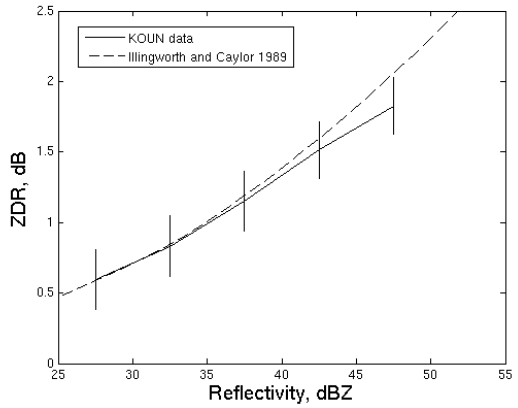

Figure 17: *Z_{dr} versus Z for KOUN data (solid line) and the theoretical curve given in Illingworth and Caylor (1989). The vertical bars represent one standard deviation of the KOUN data.*

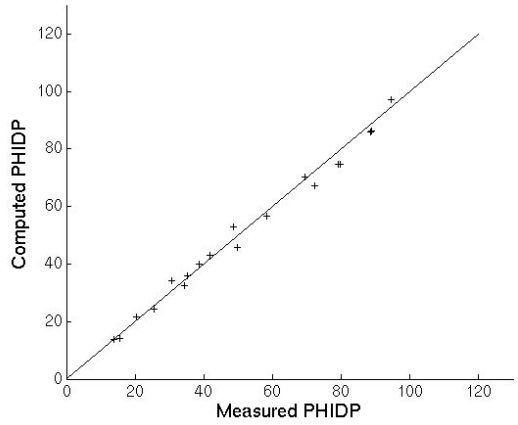

Figure 16: *Scatter plot of calculated ϕ_{dp} (from measured Z and Z_{dr}) versus measured ϕ_{dp} from TiMREX SHV data from Fig. 14 except the Z_{dr} is corrected as a function of measured ϕ_{dp} using the relationship in Fig. 15.*

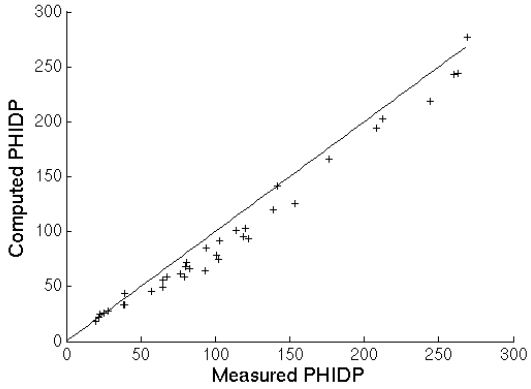

Figure 18: *Scatter plot of calculated ϕ_{dp} (from Z and Z_{dr}) versus measured ϕ_{dp} from KOUN SHV data gathered 30 March 2007. The slope of the straight line can be changed but the scatter points do not cluster symmetrically about the line. This is likely caused by antenna polarization errors.*

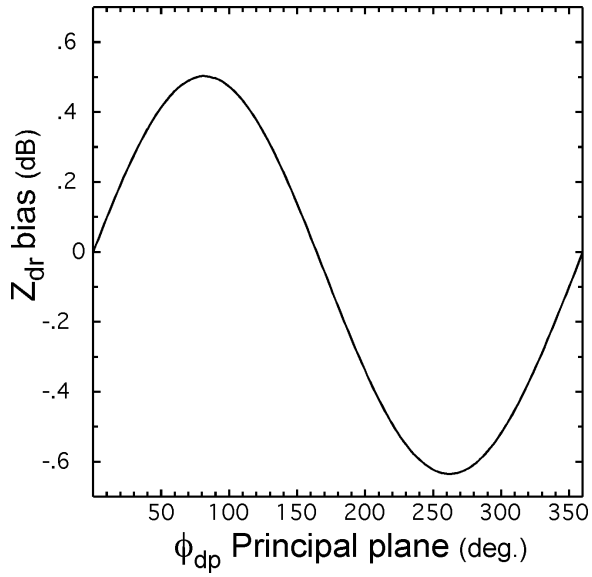

Figure 19: *SHV mode Z_{dr} bias estimated from the model for KOUN data. The antenna polarization errors are $\alpha_h = 1.7°$, $\epsilon_h = -0.7°$ and $\alpha_v = 91.7°$, $\epsilon_v = 0.7°$. The transmit polarization ellipse is characterized by $\alpha = 45°$ and $\epsilon = -30°$.*

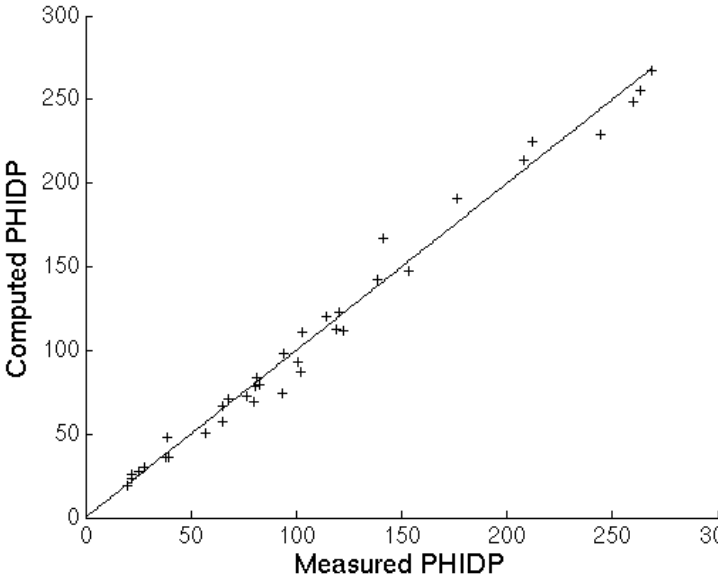

Figure 20: *Scatter plot of calculated ϕ_{dp} (from Z and Z_{dr}) versus measured ϕ_{dp} from KOUN SHV data gathered 30 March 2007 similar to Fig. 18 except the Z_{dr} data have been corrected using the Z_{dr} bias curve from Fig. 19.*

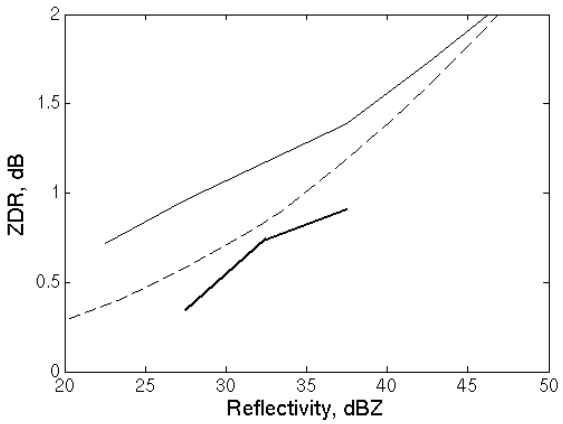

Figure 21: *Scatter plot of SHV mode Z_{dr} versus Z from KOUN data gathered 30 March 2007. The thin(thick) solid line shows data with ϕ_{dp} less than(greater than) 175 degrees and the dashed line is the relationship of Illingworth and Caylor (1989). The data have been calibrated based on data with low accumulated ϕ_{dp}, corrected for attenuation and differential attenuation, but have not been corrected for antenna polarization errors.*

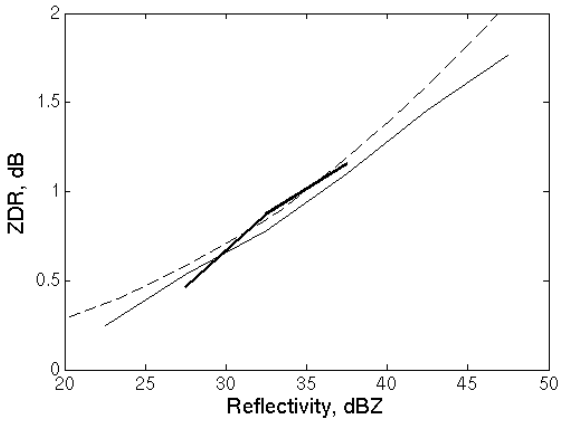

Figure 22: *Scatter plot of calculated of SHV mode Z_{dr} versus Z from KOUN data gathered 30 March 2007. Similar to Figure 21 except the data were corrected for antenna polarization errors.*